Numerical prediction of particle transport passed through ventilator by CFD with Lagrangian method

Nguyen Lu Phuong[1], Kazuhide Ito[2], Shigeki Onishi[1, 3]

[1]Interdisciplinary Graduate School of Engineering Science, Kyushu University

6-1 Kasuga-koen, Kasuga, Fukuoka, 816-8580 Japan

[2]Associate Professor, Dr.Eng.

Interdisciplinary Graduate School of Engineering Science, Kyushu University

[3]Mitsubishi Electric Corporation

Abstract

The use of CFD technique for predicting the properties of airflow fields and particle movement is effective to carry out parametric study intended for a wide range of particle sizes. In this study, particle dispersions due to turbulent flow and thermophoretic effect were analyzed for a simplified ventilator model. Numerical results that comprise a classification of particle motion, temperature difference and particle diameter were reported. The residence time of particles in the ventilator was confirmed to depend on temperature differences and particle sizes under the condition of constant supply inlet velocity. Large particles (100 μm) were strongly affected by gravitational force and settling to the inlet opening located lower part of the ventilator while smaller particles (10 μm) tended to follow the convective air streamlines. Particle removal by gravitational settling has possibilities by optimizing the flow path and velocity in the ventilator as functions of the target particle size.

Keywords

Computational fluid dynamics, Suspended particle, Lagrangian approach, Ventilation system, Vertical duct, Indoor environment.

Introduction

Indoor air can play a significant role in the transmission of various contaminants and infiltration of a ventilator may be one of the dominant transport routes of contaminants from outdoors to indoors. In particular, adverse health effects of particulate matter, such as aerosolized infectious agents, organic aerosols and yellow sand, are of increasing concern with the increase in allergic diseases.

In order to prevent contamination of particulate matter in indoor environments, the control of the transmission of particles from outdoors to indoors through ventilators is important. Toward this end, the overarching objective of this study is to analyze particle movement in a vertical ventilation duct connected with a ventilator under various boundary conditions.

Particle movements in a ventilation duct are normally affected by flow fields causing pressure differences, thermal conditions between warm and cold zones, gravitational force or by the characteristics of the particles themselves.

In summer, the side of a vertical ventilator that faces the outdoor environment develops a relatively high temperature while the other side of the ventilator facing the indoor environment may be maintained at a relatively low temperature owing to the air-conditioning system. In winter, the outdoor surface of the ventilator becomes relatively cold while the indoor surface of the ventilator is kept warm. These temperature differences between outdoor side and indoor side

of a vertical ventilator or a ventilation duct play an important role in the transportation phenomenon of particles.

Particles with different sizes have different aerodynamic mechanisms, so the behavior of dispersed particles of 10 μm and 100 μm is reported in this paper.

From the viewpoint of effective separation or removal of particles from outdoor air in ventilators and ducts, it is important to analyze the particle transport phenomenon when particles pass through a ventilation duct connected with a ventilator under various flow fields and thermal conditions.

Outline of Target Vertical Ventilation Duct Connected with Ventilator

The outline of the target vertical ventilation duct connected with a ventilator is presented in Figure 1. The target ventilator consists of two parts: a vertical ventilation duct with dimensions L × W × H = 100 × 100 × 2200 mm and a horizontal ventilator with dimensions 700 × 200 × 200 mm. The wall surface of the vertical ventilation duct faces the outdoor environment and the other faces the indoor environment. The horizontal ventilator is set in the ceiling of a residential room.

In this analysis, particles are introduced from an inlet opening of the vertical ventilation duct and transported indoors through the horizontal ventilator.

Research Methodology

Turbulent Model and Numerical Methods

The computational fluid dynamics (CFD) technique was used to predict both air flow and particle behavior. The Navier-Stokes governing equations were discretized by a finite-volume-based commercial CFD code ANSYS/ FLUENT 12. Steady flow fields were analyzed using the low Reynolds number-type k-ε model (Abe Kondo Nagano model). The QUICK scheme was used for the convection term, and a SIMPLE algorithm was used. To analyze the flow field in the boundary layer, the center of the computational cells closest to the wall surface should be at a non-dimensional distance (wall unit) of $y^+<1$, where $y^+ = u^* y_1/\nu$ and y_1 is the distance normal to the wall surface, ν is the kinematic viscosity and $u^* = \sqrt{\tau_w/\rho}$ is the friction velocity. Here, ρ is the air density and τ_w is the wall shear stress.

Flow fields in the ventilator were analyzed by Eulerian approach.

Boundary Conditions

A uniform free stream velocity of 0.3 m/s and *TI*= 5% of air flow were applied for supply inlet boundary conditions. On the solid surfaces no slip boundary condition was applied. For temperature conditions, three types of conditions were set: isothermal, summer and winter conditions. For the wall surface of the outdoor side of the ventilation duct considered here, t_w=40 °C in summer season and t_w=5 °C in winter season, while the indoor wall surface was kept at 25 ℃ in both seasons. The inlet air temperatures were t_{air} = 30 ℃ in summer and t_{air} = 0 ℃ in

winter. The temperature differences between the indoor and outdoor wall were Δt_{summer} = 15 ℃ and Δt_{winter} = 20 ℃. Other wall surfaces of the vertical ventilator were assumed to be adiabatic.

Particle Tracking Method

The Lagrangian method is applied to predict the trajectory of discrete phase particles. The particle transport in fluid flows is treated as a discrete phase made of spherical particles, which are dispersed in the continuous phase. The particle volume loading is usually assumed to be negligible, so that particles have no feedback effect on the carrier gas and particle-particle interactions are also neglected. The Lagrangian approach starts from solving the transient momentum equation for each particle:

$$\frac{d\vec{u}_p}{dt} = \vec{F}_D\left(\vec{u} - \vec{u}_p\right) + \vec{F}_g + F_T \qquad (1)$$

The first term on the right-hand side, $\vec{F}_D\left(\vec{u} - \vec{u}_p\right)$, is the drag force per unit particle mass and u is the fluid phase velocity, while u_p indicates particle velocity. F_D is expressed as follows:

$$\vec{F}_D = \frac{18\mu}{\rho_p D_p^2} \cdot \frac{C_D \cdot Re_p}{24} \qquad (2)$$

Here, μ is the molecular viscosity of the fluid, ρ is the air density, ρ_p is the density of the particle, and D_p is the particle diameter. Re_p is the Reynolds number defined using fluid viscosity μ as follows:

$$Re_p = \frac{\rho \left| \vec{u}_p - \vec{u} \right| D_p}{\mu} \tag{3}$$

C_D in equation (2) is the drag coefficient, which can be derived from

$$C_D = \frac{24(1-1.6807)Re_p^{0.6529}}{Re_p} - \frac{0.8271 \cdot Re}{8.8798 + Re_p} \tag{4}$$

$\overrightarrow{F_g}$ represents the force of gravity and is presented in equation (5).

$$\vec{F}_g = \frac{(\rho_p - \rho)}{\rho_p} \vec{g} \tag{5}$$

Particle motions in the flow field with a temperature gradient are affected by an external force proportional to the temperature gradient; this phenomenon is known as thermophoresis, F_T.

$$F_T = -D_{T,p} \frac{1}{m_p T} \frac{\partial T}{\partial x} \tag{6}$$

Here, $D_{T,p}$ denotes the thermophoretic coefficient, which can be defined as follows:

$$D_{T,p} = \frac{6\pi d_p \mu^2 C_s \left(K + C_t K_n\right)}{\rho \left(1 + 3C_m K_n\right)\left(1 + 2K + 2C_t K_n\right)} \tag{7}$$

where K_n is Knudsen number (= $2\lambda/d_p$), λ is mean free path of the fluid, K indicates the ratio of thermal conductivity of fluid and thermal conductivity of particle, m_p is particle mass, and T is local fluid temperature. C_S, C_t and C_m are model parameters and set as 1.17, 2.18 and 1.14, respectively, in this study.

In order to reproduce the particle turbulent dispersion due to turbulent fluctuations in the flow, discrete random walk (DRW) model is adopted. Turbulent fluctuations in the flow field are represented by defining an instantaneous fluid velocity.

$$\vec{u}_i = \vec{u}_i + u'_i \tag{8}$$

$$u'_i = \sigma\sqrt{2k/3} \tag{9}$$

Here, σ is a normally distributed random number; k is the turbulent kinetic energy. Previous studies have confirmed that the isotropic DRW model is effective and accurate in modeling particle dispersion and distribution in various flows (Lai and Chen, 2007; Zhang and Chen, 2007).

In this analysis, a total 10,000 particles were injected instantaneously (one-shot) at a lower part of the duct (y=100 mm) and assumed to have zero initial velocity. Particle concentrations were assumed to be low enough to ignore particle-particle interactions. Particle tracking was carried out for 30 seconds using pre-analyzed steady flow fields. The wall deposition of particles was not considered. The details of particle parameters are described in Table 1.

Cases Analyzed

Cases analyzed in this study are shown in Table 1. A total of six cases were set using parameters of particle diameter (d_p=100 μm, 10 μm) and temperature condition ($\Delta t_{isothermalr}$ = 0 ℃, Δt_{summer} = 15 ℃ and Δt_{winter} = 20 ℃).

Results and Discussion

Flow and Temperature Field

Henceforth, we focus on the results for targeting the vertical ventilation duct due to limitations of space.

Figure 2 denotes the results of velocity distribution at a vertical section of the ventilation duct in three temperature conditions and normalized velocity magnitude of air flow at the central line at y=1600 mm, z=50 mm, is presented in Figure 3. The air flow from supply inlet of the lower part to exhaust outlet of the upper part was formed in the vertical duct for the three cases. For isothermal condition, a flow field similar to a simple channel flow was formed. Concerning the summer and winter cases, upward flow was accelerated by a buoyancy effect in the wall on the high-temperature side and the air stream spread out slightly and followed the wall surface of the duct in an upward direction owing to the Coanda effect. In the region of an L-type bend in the vicinity of the exhaust outlet, separation and re-circulation flow were observed.

The temperature distributions in the ventilator at the central line (y=1600 mm, z=50 mm) are presented in Figure 4. A downward trend of temperature from the hot surface to the cool surface in summer was confirmed. In the case of winter, the supply air temperature was set at 0 °C and then the temperature profile in a crosswise (x) direction became convex downward. Combining

Figures 2, 3 and 4, the impact of temperature gradient against a flow field in the vertical ventilation duct was confirmed.

Path Line of Particle Tracking

Figure 5 illustrates the path line of 30 representative particles of Case 1-1, Case 2-1 and Case 3-1 (cases of D_p= 100 µm). The particle motion at a size of 100 µm was governed by gravitational settling and injected particles were not transported toward the exhaust outlet, which was located in the upper part of the domain. As shown in Figure 5, some of the particles near the left surface dropped down right away after the injection and were directly transported to the supply inlet opening located in the lower part of the ventilation duct. Meanwhile, the rest of them on the right surface were accelerated by inertial force and subsequently fell down to the injection surface by gravitational settling.

Figure 6 shows the spatial distribution of path line of 30 representative particles of Case 1-2, Case 2-2 and Case 3-2 (cases of D_p= 10 µm). While the majority of the particles with D_p= 100 µm were exhausted through the supply inlet opening, the particles with D_p=10 µm tended to follow a streamline of carrier air flow and were transported toward the upper part of the duct. Generally, the small particles (D_p=10 µm) moved in accordance with the convective flow of air, and the effect of the discrete random walk model was relatively prominent compared with thermophoresis for particle motion. The influence of temperature gradient on particle motion was not clear in this analytical condition.

Particle Residence Time in Duct

Residence time of particles inside the vertical ventilation duct is one of the most important parameters of particle motion. This residence time of each particle was counted from injection time (t=0) until leaving the domain or reaching the maximum time step. Figure 7 indicates the residence times of particles in comparison with nominal time constant of gas stream τ_n in six cases. τ_n is defined by the volume of the device [m^3] and the supply air flow rate [m^3/s]. Figure 7 a) denotes the results of small particles (D_p=10 μm) and a large amount of particles stayed in the ventilation duct longer than the nominal time constant (τ_n=7.7 sec). In Cases 1-1, 2-1 and 3-1, the percentages of exhausted particles from the ventilation duct at the point of nominal time constant τ_n were 27.7% in the isothermal case, 29.3% in the summer case and 25.5% in the winter case. Small particles (D_p=10 μm) took longer than τ_n to pass through the vertical duct. At t=30 sec from particle injection, the percentages of exhausted particles from the ventilation duct were 70% for Case 1-2 (isothermal), 73% for Case 2-2 (summer) and 67% for Case 3-2 (winter). At this time point, there remained a number of particles in recirculation or a stagnant region in the duct. Moreover, the number of particles in Case 1-2 (summer) that had left the domain was greater than those of 2-2 and 3-2 at the same residence time. One of the reasons for this difference was that the difference of flow field caused buoyancy and thermophoresis caused a temperature gradient.

Figure 7 b) shows the results of relatively large particles (D_p=100 μm) for staying time in the vertical duct. In this case, the residence times of most particles were shorter than the nominal time constant τ_n because the gravitational force became dominant and acted downward and then particles passed through the supply inlet opening quickly. The percentages of exhausted particles

from the supply inlet opening located in the lower part of the ventilation duct at the point of nominal time constant τ_n were 93.9% for Case 1-1 (isothermal), 94.6% for Case 2-1 (summer) and 92.7% for Case 3-1 (winter).

For a representative inspection plane, 8 plane surfaces (x-z plane) at heights of y=350 mm, y=600 mm, y=850 mm, y=1100 mm, y=1350 mm, y=1600 mm, y=1850 mm, and y=2100 mm were created to compare the particle information like instantaneous velocity, temperature, mass flow, and residence time of particle. Figure 8 a) and 8 b) indicates the distribution of mean velocity components (*u* of *x*-direction, *v* of *y*-direction) of all of the particles passing each inspection plane during the calculation time (30 sec). The values were normalized by inlet air velocity (U_{in}= 0.3 m/s). Although the difference of *u*-velocity component of particles in summer and winter conditions is not significant, the discrepancy between the results of the isothermal condition and the other two cases (summer and winter) indicates the effect of temperature differences: buoyancy and thermophoretic force as shown in Figure 8 a). In Figure 8 b), the mean *v*-velocity component in summer can be seen to increase owing to buoyancy effect from the air flow.

From Figure 8 c), which denotes the average temperature of all of the particles passing each inspection plane during the calculation time (30 sec), the average temperature of particles can be seen to gradually increase along with updraft and the temperature differences between lower plane (y=350 mm) and upper plane (y=2100 mm) were 1.7 °C in summer and 7.7 °C in winter.

Conclusions

CFD modeling of convective air flow and particle motion in a ventilation device heated by a seasonal condition has been presented in this paper. The Lagrangian approach has been used to compute particle trajectories, concentration distributions and residence time of particles in the ventilator. The temperature gradient between hot and cold wall surfaces greatly influenced air flow pattern and temperature distribution, and had a certain impact on particle movement. Small particles (D_p=10 μm) were likely to follow the air flow while large particles (D_p=100 μm) were deposited and exhausted through the supply inlet opening.

Analyses for other particle size, flow and temperature conditions are future research work.

Acknowledgement

This research was partly supported by a Grant-in-Aid for Scientific Research (JSPS KAKENHI for Young Scientists (S), 21676005). The authors would like to express special thanks to the funding source.

References

(1) FLUENT, 2006. Fluent 6.3 User's guide. Fluent Inc., Lebanon.

(2) Abe, K., Kondoh, T., Nagano, Y. A new turbulence model for predicting fluid flow and heat transfer in separating and reattaching flows—I. Flow field calculations, Int. J. Heat Mass Transfer 37 (1) (1994) 139–151.

(3) Lai, A.C.K., Chen, F.Z., 2007. Comparison of a new Eulerian model with a modified Lagrangian approach for particle distribution and deposition indoors. Atmospheric Environment 41, 5249–5256.

(4) Zhang, Z., Chen, Q., 2007. Comparison of the Eulerian and Lagrangian methods for predicting particle transport in enclosed spaces. Atmospheric Environment 41 (25), 5236–5248.

(5) Zhang, Z. and Chen, Q. 2009. Prediction of particle deposition onto indoor surfaces by CFD with a modified Lagrangian method, Atmospheric Environment, 43(2), 319-328.

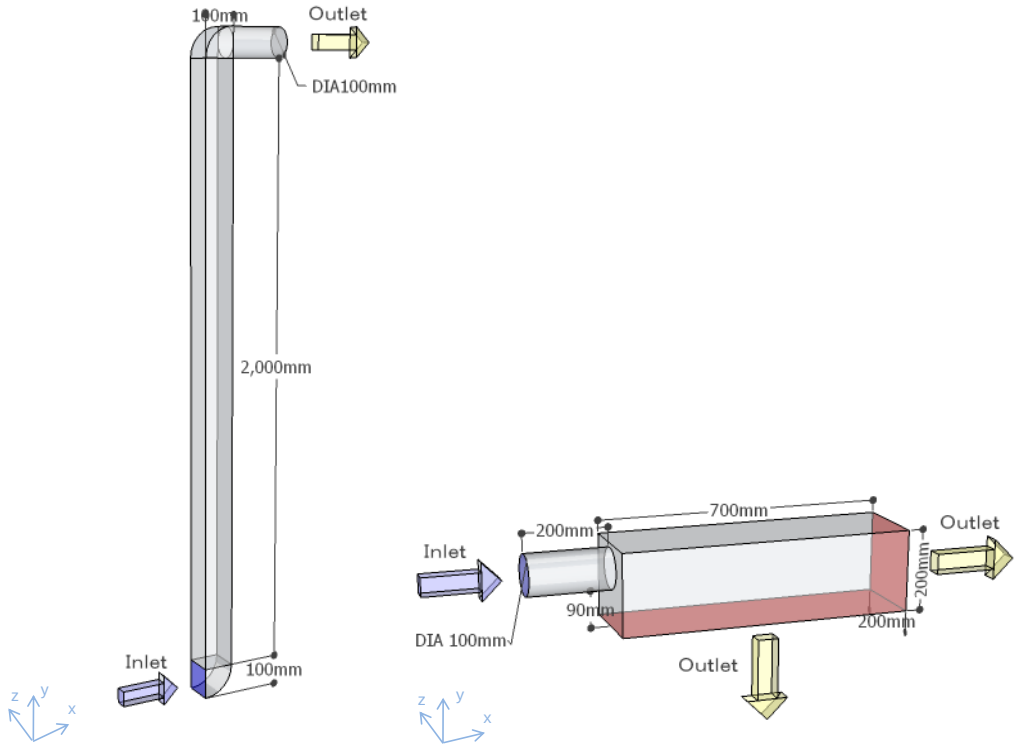

(1) Vertical ventilation duct (2) Horizontal ventilator

Figure 1 Outline of target ventilator

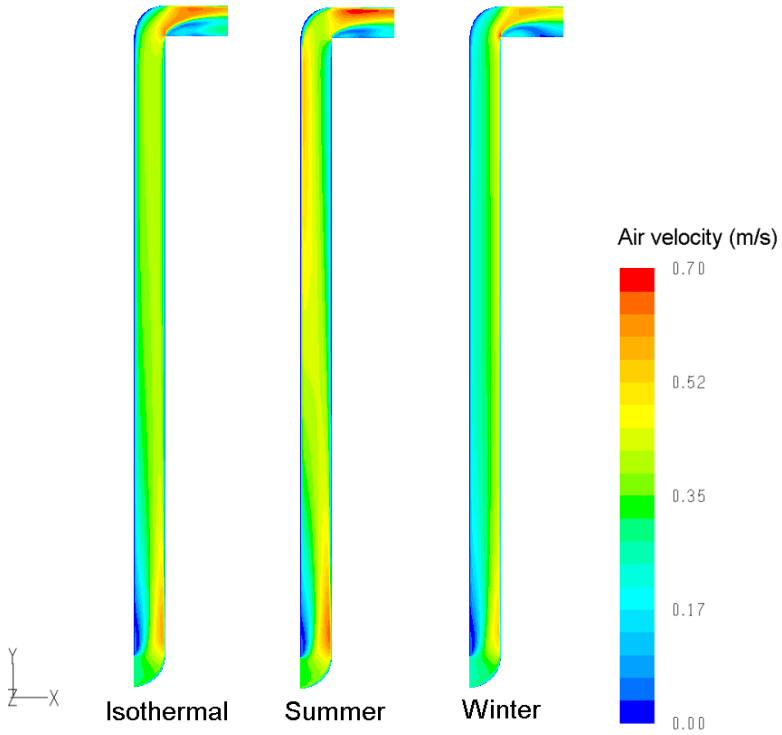

Figure 2 Velocity magnitudes inside the vertical ventilator (m/s)
(*x*-*y* plane at the center of spanwise (z=50 mm) direction)

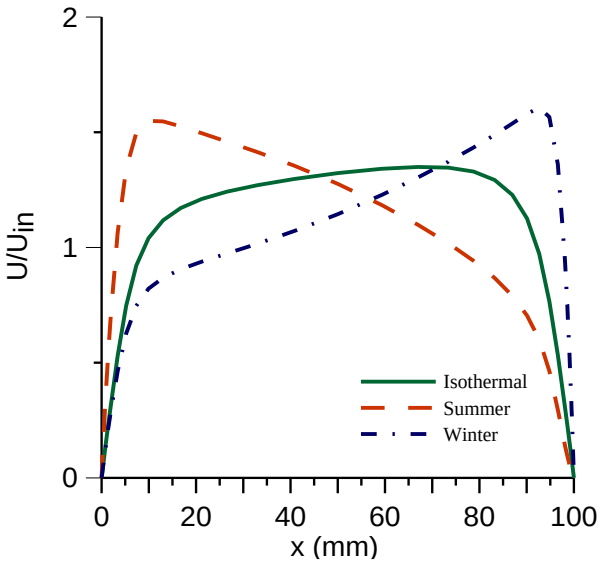

Figure 3 Normalized velocity magnitude of air flow along *x* direction (at y=1600 mm, z=50 mm)

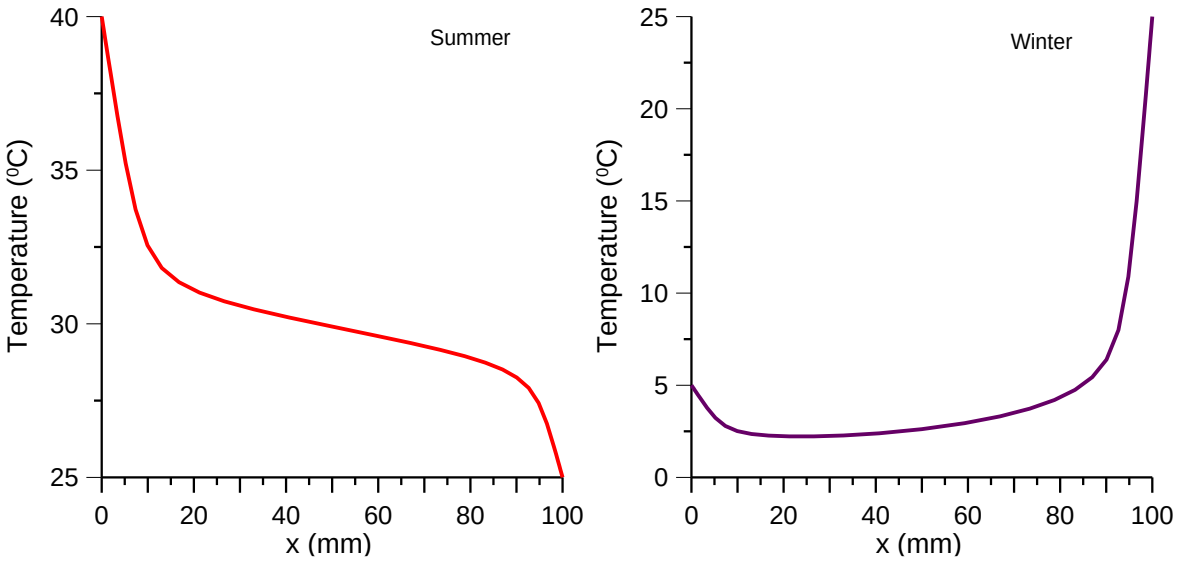

Figure 4 Temperature distribution along *x* direction at y=1600 mm, z=50 mm, in summer (left side fig.) and winter (right side fig.).

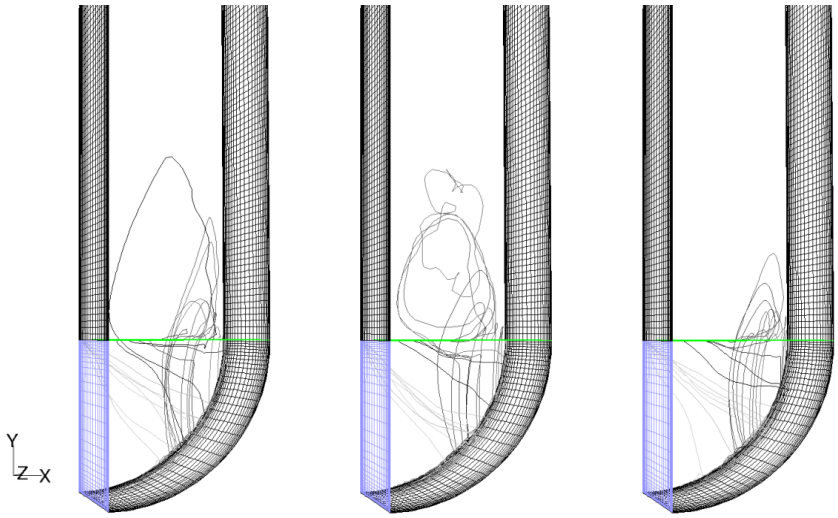

a) Case 1-1 (isothermal) b) Case 2-1 (summer) c) Case 3-1 (winter)

Figure 5 Predicted path line of particles (D_p= 100 µm) in the ventilator

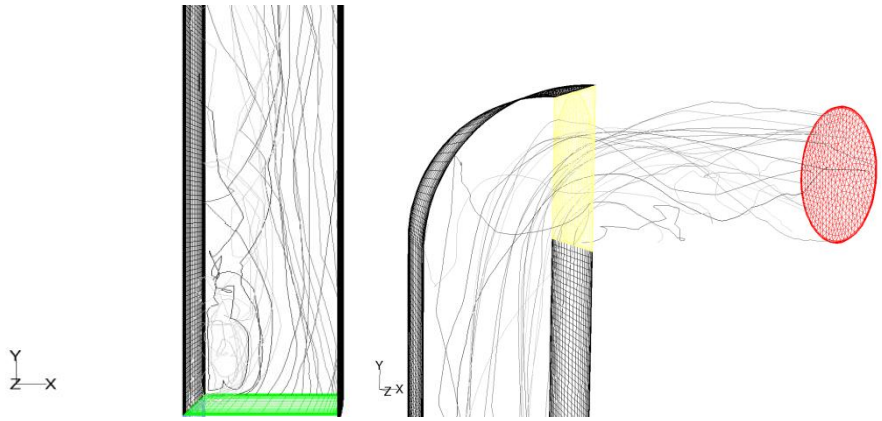

a) Case 1-2 (isothermal)

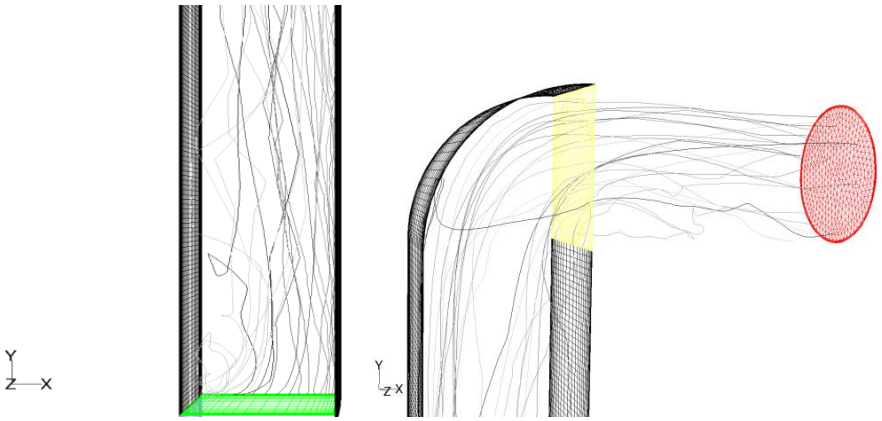

b) Case 2-2 (summer)

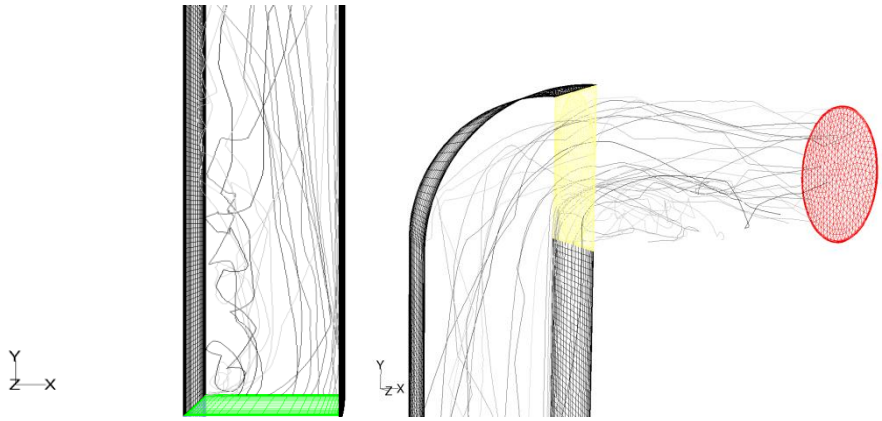

c) Case 3-2 (winter)

Figure 6 Predicted path line of particles (D_p= 10 μm) in the ventilator in the vicinity of inlet (left side fig.) and outlet (right side fig.) of ventilator

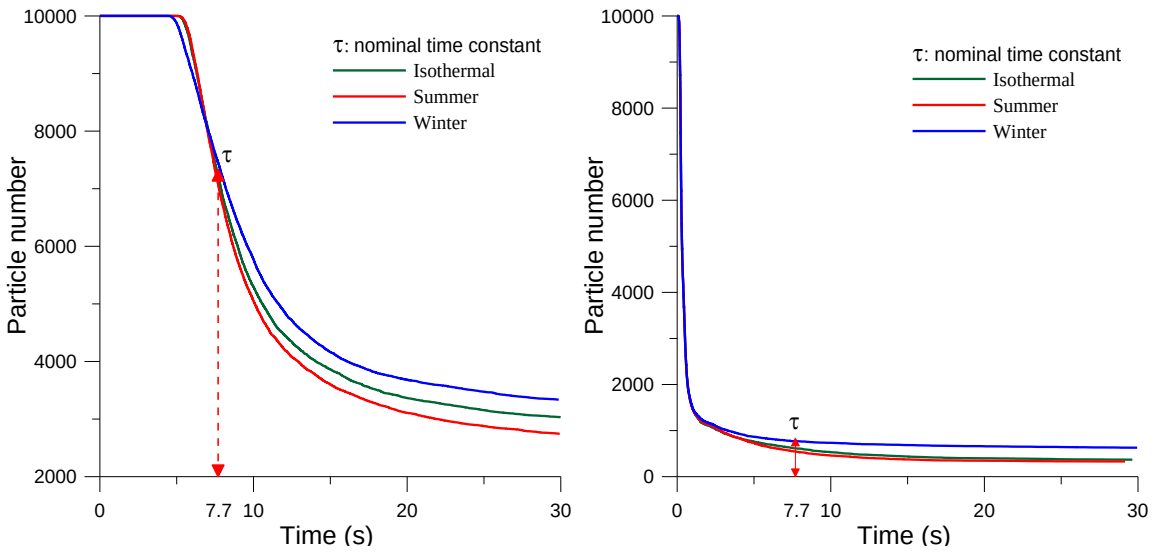

a) Particle size of 10 μm b) Particle size of 100 μm

Figure 7 Residence time of particles in the vertical ventilation device

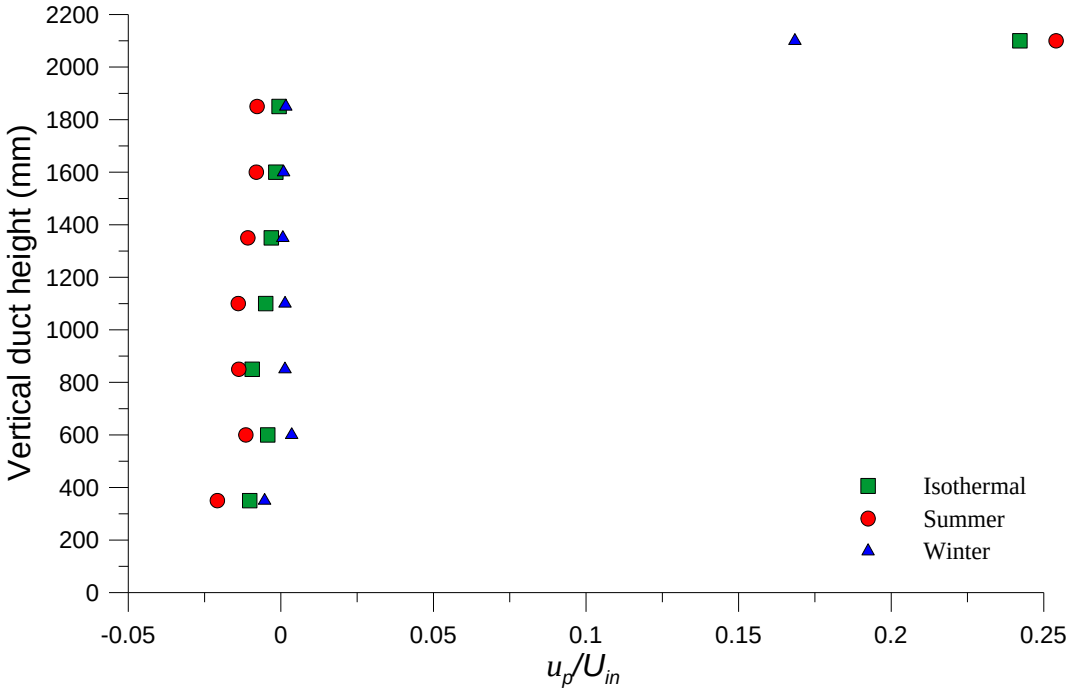

a) Distribution of the mean particle velocity component *u* of *x*-direction at 8 y-planes

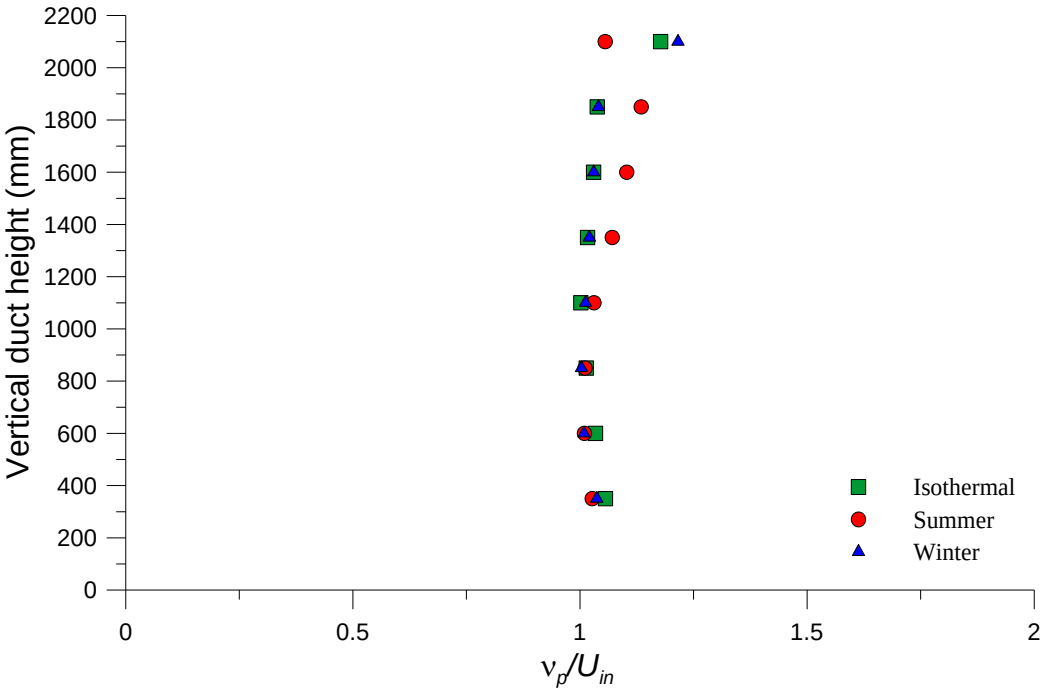

b) Distribution of the mean particle velocity component *v* of *y*-direction at 8 y-planes

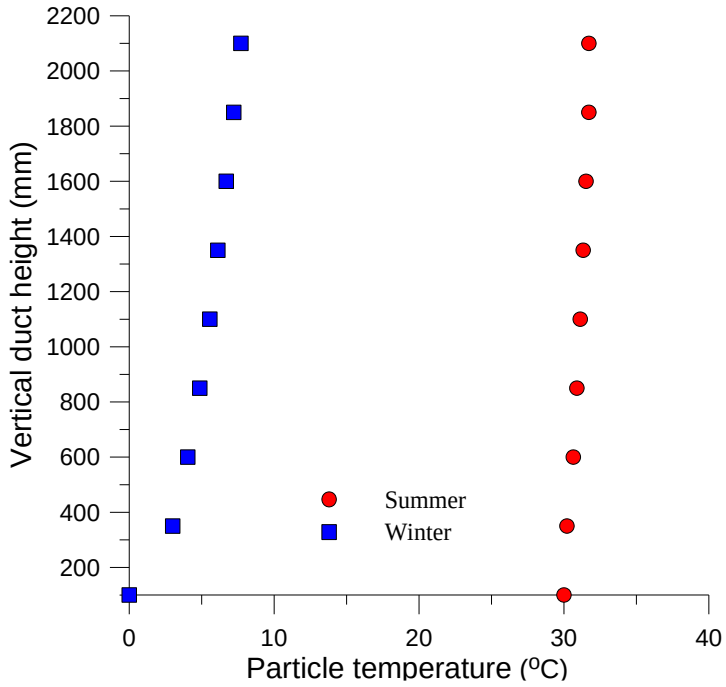

c) Distribution of the mean particle temperature at 8 y-planes

Figure 8 Distribution of mean velocity component (*u*, *v*) and temperature of particles along the vertical ventilator

Table 1 Cases analyzed

Case	Temperature condition	Particle properties
Case 1-1	Isothermal	D_p=100[μm],ρ_p=9.93×10^2[kg/m^3], 520 [ng/particle]
Case 1-2		D_p=10 [μm], ρ_p=9.55×10^2[kg/m^3], 0.5 [ng/particle]
Case 2-1	Summer	D_p=100[μm],ρ_p=9.93×10^2[kg/m^3], 520 [ng/particle]
Case 2-2		D_p=10 [μm], ρ_p=9.55×10^2[kg/m^3], 0.5 [ng/particle]
Case 3-1	Winter	D_p=100[μm],ρ_p=9.93×10^2[kg/m^3], 520 [ng/particle]
Case 3-2		D_p=10 [μm], ρ_p=9.55×10^2[kg/m^3], 0.5 [ng/particle]